MEKATRONIKA: JOURNAL OF INTELLIGENT MANUFACTURING AND MECHATRONICS
E-ISSN: 2637-0883
VOLUME 8, ISSUE 1, 2026, 43 - 49
DOI: https://doi.org/10.15282/mekatronika.v8i1.13853

UNIVERSITI MALAYSIA PAHANG AL-SULTAN ABDULLAH

RESEARCH ARTICLE

# Experimental investigation of traction forces in Touyoura sand using a C-shaped grouser

**Mochamad Edoward Ramadhan[1], Ahmad Najmuddin Ibrahim[2]*, Yasuhiro Fukuoka[3]**

[1]Mechanical Engineering Department, Faculty of Engineering, University of Jember, Jember 68121, Indonesia
[2]Faculty of Manufacturing and Mechatronic Engineering Technology, Universiti Malaysia Pahang Al Sultan Abdullah, Pekan Campus 26600, Pahang, Malaysia
[3]Department of Mechanical System Engineering, Ibaraki University College of Engineering, Ibaraki University Hitachi 316-8511, Japan

**Abstract –** Exploration rovers on Mars and the Moon frequently encounter wheel entrapment in loose terrain due to insufficient traction, which compromises mobility and mission success. Enhancing wheel traction is critical, and the integration of grousers has been empirically demonstrated to improve performance through complex wheel–terrain and grouser–terrain interactions. Traditional measurement methods, such as the bevameter, are designed for heavy vehicles and are less suitable for lightweight planetary rovers. This study introduces a simplified traction measurement prototype utilizing a static shaft connected to a 5-kg load cell and a C-shaped grouser with a width of 90 mm and a physical height of 150 mm with an effective immersion length of 100 mm. During experimental trials, the prototype penetrated Toyoura sand as the wheel advanced, enabling direct traction measurement over a distance of 170 mm. Results indicate that clockwise rotation with the lateral side facing forward generates a traction force of 20.3 N, while a backward orientation yields 22.7 N. The average traction force per grouser cycle ranges from 20.11 to 22.90 N, with a mean of 21.5 N and a standard deviation of 1.3, confirming high reproducibility. The effective attack angle was determined to be 140.16°, facilitating gradual soil shear mobilization without inducing excessive sinkage. These findings suggest that while grouser orientation influences peak forces, the differences remain relatively minor, with the lateral sides primarily serving as structural reinforcement for the C-shaped geometry.

**Article History**
Received : 20 January 2026
Revised : 13 April 2026
Accepted : 9 June 2026
Published : 30 June 2026

**Keywords**
*Planetary rover*
*Traction force*
*C-shaped grouser*
*Wheel-terrain interaction*
*Toyoura sand*

## 1. Introduction

The development of rovers for exploration on Mars and the Moon continues to advance rapidly. These rovers frequently encounter terrain composed of loose sand and jagged rocks, which often leads to wheel entrapment, a critical failure mode in which loss of traction prevents further movement. To mitigate these mobility risks, the integration of grousers onto rover wheels has become a standard approach. Early studies by Kubota et al. [1] demonstrated that rectangular and spiral grousers significantly enhance traction, although the specific performance trade-offs associated with these distinct geometries were not exhaustively analyzed. Beyond experimental work, researchers like Ishigami et al. [2] have developed terramechanics-based models to decouple longitudinal and lateral traction components, providing a theoretical foundation for rover control on loose soil. Subsequent investigations have focused on the influence of grouser geometry on climbing performance. Nakashima et al. [3] found that 5- and 20-mm grousers were insufficient for slopes exceeding 20°, suggesting that grouser height must be strategically adapted to the intended terrain slope. Building upon these findings, Irani et al. [4] established a validated dynamic terramechanics model for rigid wheels, applicable to both planetary and terrestrial robots operating in loose sandy environments. To address the limitations of earlier models, Sutoh et al. [5]– [6] examined the interplay among rover mass, wheel dimensions, and surface patterns. Their results indicated that while increasing mass does not fundamentally alter terrain interaction mechanisms, it can degrade overall wheel efficiency. Furthermore, they emphasized that grouser spacing and height are vital to ensuring that multiple grousers maintain contact within the critical soil interaction angle. Recent analysis has also focused on uneven load distribution and soil-stress dynamics. Zhou et al. [7] noted that higher loads and slip interactions on uneven surfaces can lead to rapid sand displacement, while Higa et al. [8] experimentally mapped the two-dimensional normal stress at the wheel–terrain interface, identifying a characteristic bell-shaped distribution. Additionally, studies by Du et al. [9] and Jiang et al. [10] have quantified how traction efficiency decreases with higher vertical loads and lower soil density yet improves significantly with the addition of grousers. Notably, Higa et al. [11] later posited that grousers dominate nearly all traction components, challenging traditional assumptions regarding the role of the wheel surface. This shift in understanding has led to detailed comparisons of grouser shapes, with trapezoidal and inclined geometries often outperforming standard rectangular designs on flat sandy surfaces. Inotsume et al. [12] investigated the effects of grouser number, height, orientation, and end caps under longitudinal and lateral slip conditions, showing that increasing grouser height had a similar effect to increasing wheel slip.

As wheel designs evolve toward hybrid mobility and deployable mechanisms, high-fidelity simulations have begun to accurately reproduce experimental resistive forces and sinkage with minimal error. The traction force that occurs between the grouser wheels and the ground is the most significant object of study. Experiments conducted by Ibrahim et al. [13] by placing 6 grousers on the lateral side of the rover seem to be an innovation to increase the wheel traction force along with the formation of sinkage. In addition, the study of Ibrahim and Fukuoka [14] stated that the assistive grouser they had made had better electrical energy efficiency than conventional grousers. By using modeling, Sabarudin et al.

***CORRESPONDING AUTHOR | Ahmad Najmuddin Ibrahim** | ✉ anajmuddin@umpsa.edu.my

succeeded in observing the traction force that occurs on the x and y axes of the three assistive grousers interacting with sand to cause energy efficiency from the use of assistive grousers, in addition, they also simulated the interaction of assistive grousers with declining terrain conditions [15]. However, the value of the resulting parameters has not been validated with experimental measurements; thus, Aziz et al. [16] continued the research by varying the angle of attack of the grouser. The results of the study stated that for sandy terrain with a slope of 0-20º, an angle of attack of 20º provided quite good results, while for flat terrain, an angle of attack of 0º was able to produce maximum tractive force values . Not only that. Aziz et al also conducted research on several shapes such as flat, c-shaped, and chevron. C-shaped grousers were able to provide greater traction than others. To conduct further analysis of C-shaped grousers, a parametric study by Basri et al. [13] indicated that while wider grousers increase peak forces, they may inadvertently reduce net traction, whereas inverted orientations often provide superior overall performance. Furthermore, investigations into low-speed operations by Takehana et al. [14] revealed that even at minimal speeds, heavy wheels can suffer from "bulldozing" effects and excessive sinkage on sandy terrain. These innovations culminated in the development of the Lev-1 grouser wheel, which utilises a 90° placement to enhance mobility in extreme extraterrestrial environments. Building on these rapid developments, Dong et al. [15] recently introduced a soil-ploughing wheel design utilising a C-shaped grouser, which generated a substantial drawbar force of 200 N under high vertical loads. Given the promising nature of this geometry, the present study aims to quantify and compare the traction forces of a C-shaped grouser through direct, localised terrain measurements. By mounting the grouser to a load cell on a static wheel shaft, this experimental configuration allows for the precise quantification of traction forces over a travel distance of 170 mm. This approach provides a granular understanding of the interaction mechanisms between the grouser and the terrain, offering insights into how such designs can be optimised for future lightweight planetary rovers.

## 2. Materials and Methods

This study investigates the traction force generated by a solid wheel equipped with C-shaped grousers operating on Toyoura sand under controlled laboratory conditions. All experiments were conducted indoors to minimize external disturbances, with the ambient temperature maintained between 26 °C and 28 °C and relative humidity ranging from 50% to 68%. The experimental process involved a C-shaped grouser prototype instrumented with load cells, initially positioned above the sand surface. As the wheel rotated, the grouser penetrated the sand, generating measurable displacement until it exited the soil. During the cycle, the penetration, traction, and retraction forces were continuously recorded to establish correlations with existing terramechanics models.

### 2.1 Materials

#### 2.1.1 Wheel and grouser

The test apparatus comprised a wheel tread, rim, and internal frame structure. The assembly integrated two actuation mechanisms: one for wheel rotation and another for adjusting the grouser attack angle. The wheel rim was manufactured from 6061 aluminum alloy, while the tread was fabricated from PLA components, resulting in an outer diameter of 205 mm. The wheel was equipped with six C-shaped grousers, each fabricated from a 2-mm-thick 6061 aluminum alloy plate. Each grouser had a physical height of 150 mm, a width of 90 mm, and a lateral side width of 20 mm. These grousers were mounted perpendicular to the wheel surface (90° attack angle) at a radial distance of 170 mm from the wheel center to ensure consistent soil penetration and reliable measurement of translational displacement.

#### 2.1.2 Soil properties

Toyoura sand was selected as the testing medium because of its uniform particle characteristics (0.1–0.3 mm) and prevalence in planetary terrain simulations. The bulk density of the sand was maintained between 1450 and 1600 kg/m³, with an internal friction angle ranging from 32° to 46°. The sand was housed in a test bin with a uniform depth of 150 mm, preventing any interaction between the wheel and the base of the container.

### 2.2 Equipment and Instrumentation

The experiments were conducted using a custom-built single-wheel test bed. Two load cells, each with a maximum capacity of 49 N, were mounted on the grouser shaft to capture the direct traction forces. Data acquisition was performed using an HX711 analogue-to-digital converter and an Arduino Uno microcontroller, with real-time recording handled by CoolTerm software at a time resolution of 0.01 s. To ensure signal stability, a DC voltage stabilizer provided a regulated 4–5 V supply to the sensors. Wheel rotation was driven by a Maxon RE40 DC motor (150 W) equipped with a 1088:1 reduction gear system, enabling precise low-speed rotation. The wheel speed was fixed at 1 RPM across all trials to ensure uniform loading and natural soil deformation.

### 2.3 Experimental Details

Before each trial, the sand surface was manually levelled to maintain consistent initial conditions. The wheel was positioned with the grouser tips at a clearance of 1–2 mm above the surface. Each test condition was repeated five times to evaluate reproducibility, and the average traction force from these repetitions was used for subsequent analysis. Key constant parameters included the vertical load of 12 N, the grouser attack angle of 90°, rotation speed of 1 RPM, and soil depth of 150 mm. The primary variables measured were the traction force (*N*) and resulting wheel sinkage (mm) during grouser engagement. Figure 1 shows a schematic of the experimental configuration, including the relative positions of the wheel, load cells, motor, and sand bin.

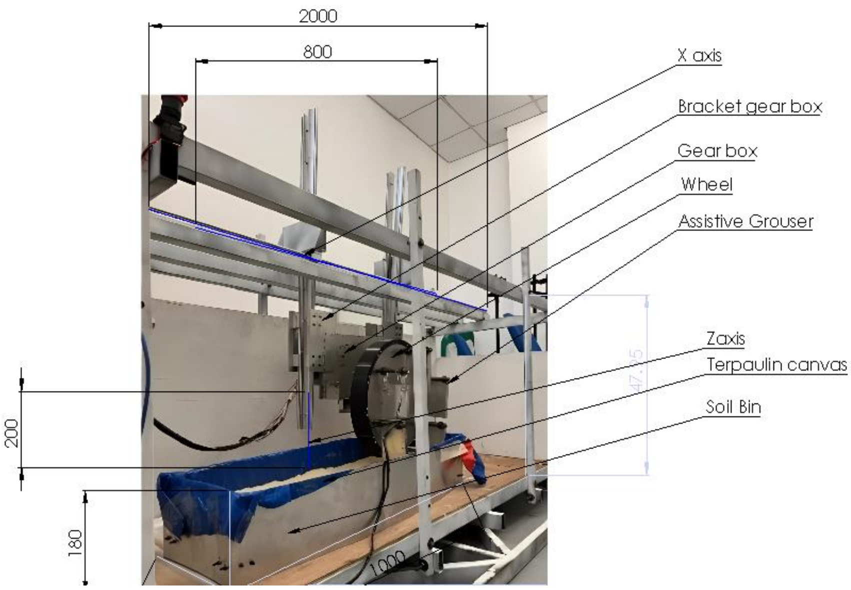


Figure 1. Single wheel test bed

## 3. Results and Discussion

### 3.1 Traction Force Profile per Grouser Cycle

The traction force profiles for the C-shaped grouser in both forward and backward lateral orientations exhibit a distinct cyclic pattern over Toyoura sand (Figure 2). Each cycle represents a single grouser's interaction over a displacement of approximately 170 mm, tracing the path from initial surface contact (U) to maximum penetration depth (B), and finally to retraction toward the surface (U'). During the initial phase, the resistance remains low as soil mobilization is minimal and the sand structure remains relatively intact. As the wheel rotates clockwise, the traction force increases progressively owing to soil deformation and localized compaction, reaching its peak at the deepest penetration point (B). Data analysis shows that the forward lateral orientation generates traction forces between 20.11 and 20.43 N, whereas the backward orientation yields significantly higher peaks ranging from 22.52 to 22.90 N. While the backward orientation maintains a peak force longer (indicated by a broader apex), the forward orientation exhibits a sharper peak, reflecting a more rapid development of traction and wheel displacement.

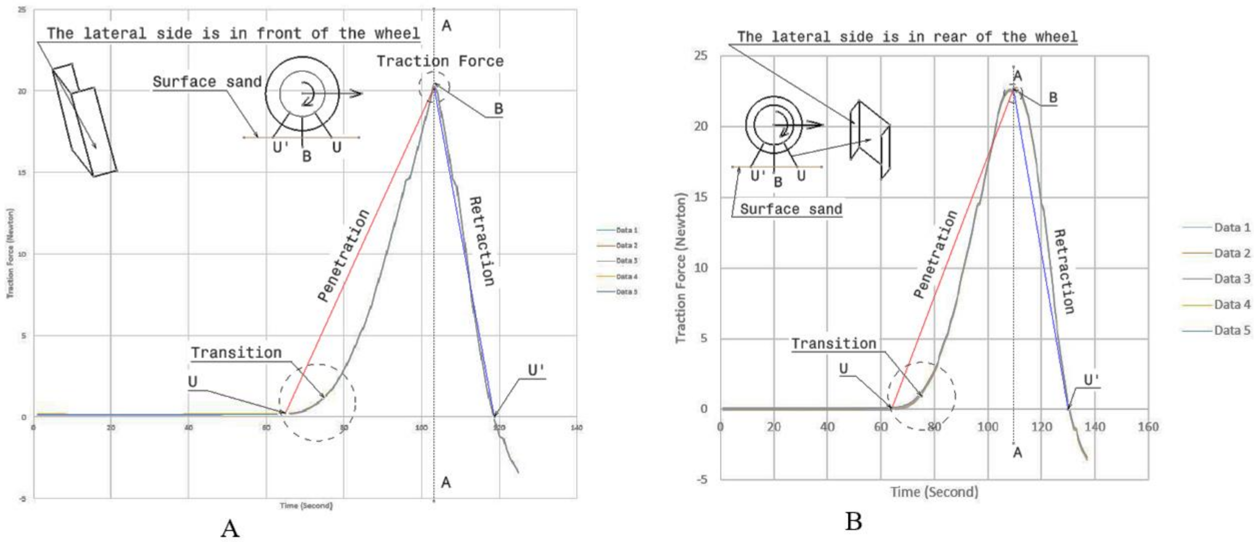


Figure 2. Traction force profile of a single C-shaped grouser: (a) lateral side positioned in front of the wheel; (b) Lateral side positioned at the rear of the wheel

### 3.2 Reproducibility and Consistency across Cycles

Experimental reproducibility was evaluated through five repetitions for each condition. For the forward orientation, the recorded profiles largely overlap, resulting in a standard deviation (SD) of 5.87 across trials. In contrast, the backward orientation showed slightly higher variability, with an SD of 7.7. When the datasets were integrated, the mean traction force was 21.5 N, with an overall standard deviation of 1.3. These results confirm that the peak and average traction values are reliable metrics for evaluating grouser performance. A scatter plot illustrating the distribution of the maximum, minimum, and average values is provided in Figure 3.

### 3.3 Effect of Grouser Geometry and Attack Angle

C-shaped grousers demonstrate superior traction compared to conventional straight designs because the lateral sides act as structural stiffeners that help retain soil and promote maximum compaction within the contact area. The curved profile ensures progressive soil penetration, which is critical for rovers with limited weight. A key finding was the effective attack angle of 140.16°, calculated from the sum of the penetration angle (50.16° from U to B) and the retraction/surface angle (90° from B to U'). This specific angle, illustrated in Figure 4, facilitates the gradual mobilization of soil shear without inducing excessive sinkage, thereby optimizing traction stability in loose granular terrain.

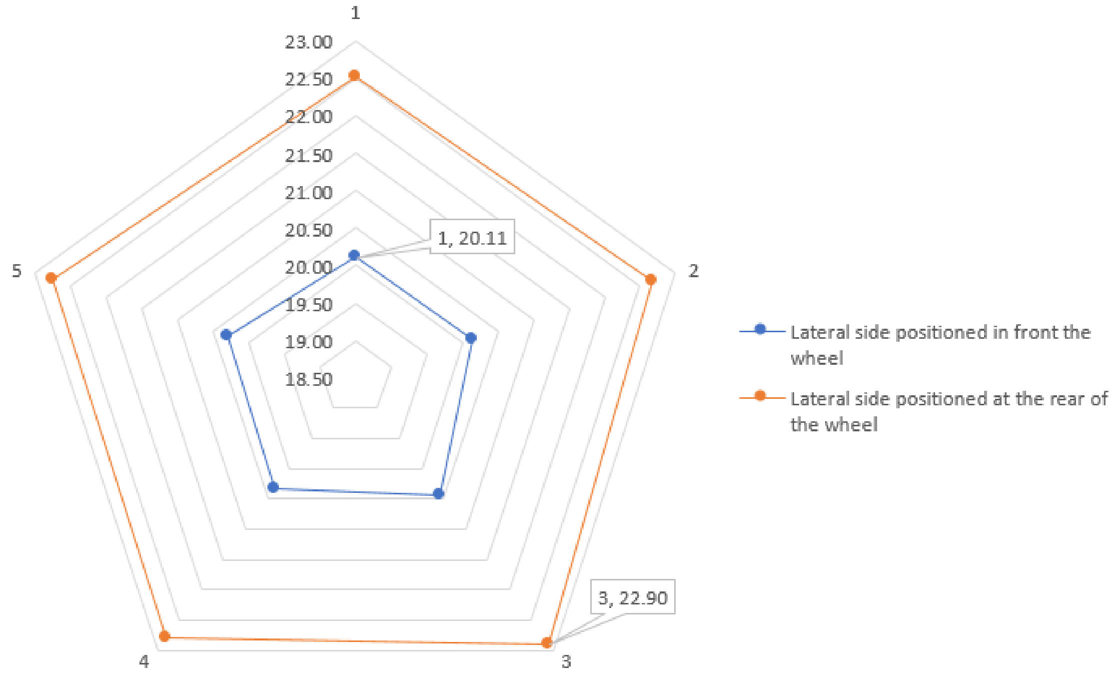


Figure 3. Presents the distribution of traction force data for both forward and backward

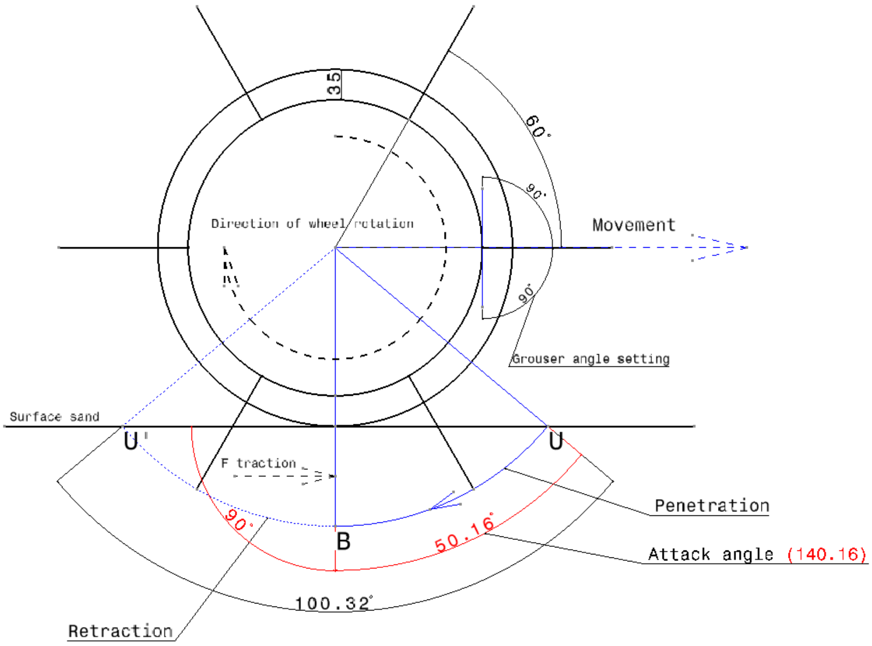


Figure 4. Angle of attack of the grouser

### 3.4 Relationship between Traction Force and Sinkage

The measured traction force strongly correlated with wheel sinkage, which ranged from 0.8 to 2 mm. Deeper penetration increased the soil-grouser contact area and shear resistance. With a contact area of 9000 mm², the average traction of 22.73 N resulted in a distributed traction force (q) of 0.0025 N/mm². Traction as a function of the effective grouser length (L) can be expressed as

$$F(L) = 0.00253 \times 90 \times L$$

For the experimental sinkage of 0.8–2 mm and L=100 mm, this yields FL =0.2277× L. The force distribution relative to the varying grouser lengths is presented in Figure 5.

### 3.5 Comparison with Previous Studies

The results were contextualized with respect to the "soil-ploughing" mechanism studied by Dong et al. [15]. While Dong et al. [15] reported a distributed traction force (q) of 0.02 N/mm², our study observed a value of 0.0025 N/mm², which is approximately one-tenth of their value. This discrepancy is attributed to the differing methodologies: Dong et al. [15] utilized a drawbar with a counterbalance system under high vertical loads (50–100 kg), whereas this study captured localized transitions during each grouser cycle under a low vertical load of 12 N. Despite the lower load, the C-shaped grouser generated comparable traction efficiency, validating its effectiveness for lightweight planetary rovers. This comparison, visualized in Figure 6, highlights that the 140.16° attack angle and curved geometry effectively mobilize shear while preventing the efficiency losses that are typically associated with excessive soil yielding.

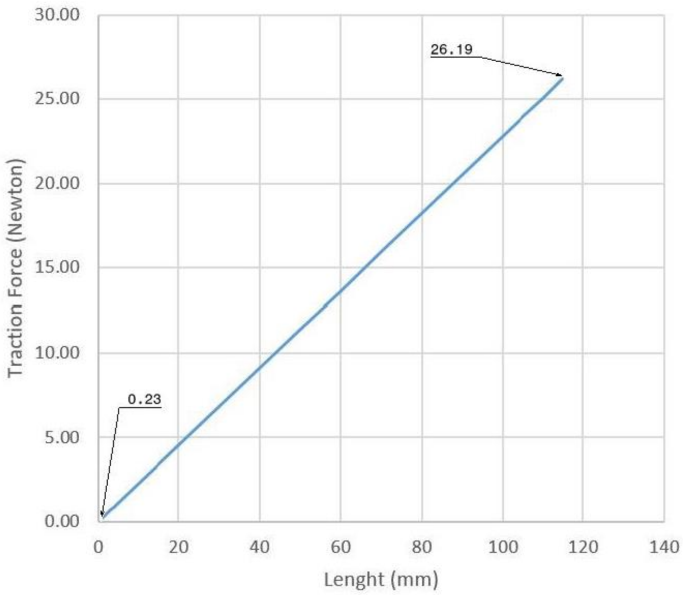


Figure 5. Force as a function of varying grouser length

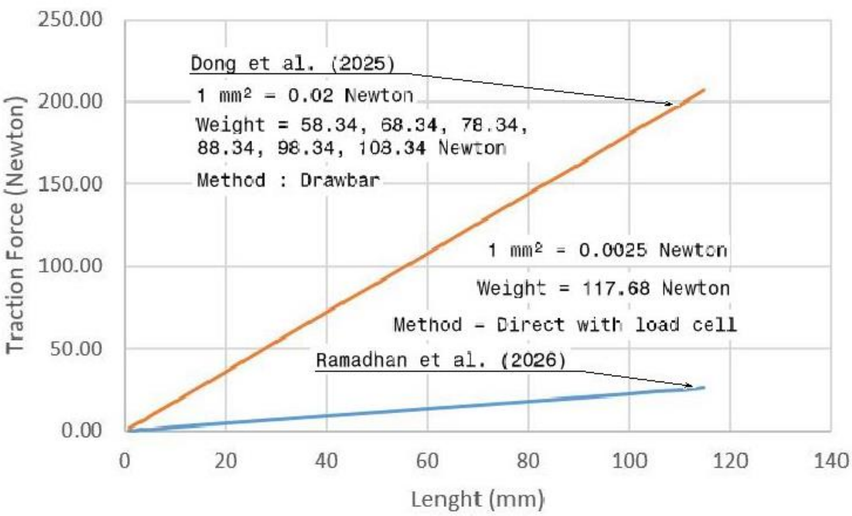


Figure 6. Comparison between soil plough and C-shaped grouser

The integration of the analyses from Sections 3.3 and 3.4 with this comparative study demonstrates that the performance of the C-shaped grouser is fundamentally governed by its geometry, effective attack angle of 140.16°, and regulated sinkage. The curved geometry facilitates progressive soil engagement, whereas the 140.16° attack angle enables effective shear mobilization without inducing excessive sinkage. Furthermore, the established correlation between traction and sinkage confirms that while moderate penetration enhances shear resistance, excessive sinkage triggers soil yielding, thereby diminishing overall efficiency. Ultimately, the cycle-resolved direct measurements used in this study capture transient interaction phenomena that are typically obscured in average-based methodologies, validating the effectiveness of C-shaped grousers on soft granular terrain and providing a robust, physically grounded framework for future wheel optimization.

## 4. Conclusions

This study investigated the traction performance of C-shaped grousers on a single-wheel test bed using Toyoura sand under a vertical load of 12 N. The experimental results indicate that the lateral side orientation has a minimal effect on the average traction force per grouser cycle, which ranged from 20.11 to 22.90 N with a mean of 21.5 N and a standard deviation of 1.3. This high level of reproducibility confirms that while minor variations in peak traction exist between front- and rear-facing orientations, the differences are not statistically significant. Consequently, the lateral side is identified as primarily functioning as a structural stiffener for the C-shaped geometry. The study further established that the effective attack angle of 140.16° enables the gradual mobilization of soil shear, thereby limiting excessive soil deformation and enhancing traction stability. Compared with previous soil-ploughing wheel designs, the C-shaped grouser delivers efficient traction even under relatively low vertical loads while maintaining consistent performance across repeated cycles. These findings highlight the significant potential of C-shaped grousers for lightweight planetary rover applications and provide practical insights for optimizing grouser geometry and orientation. Future research should aim to extend these investigations to various soil types, particularly agricultural soils, and explore alternative wheel geometries under dynamic operating conditions to further validate these findings beyond Mars and Moon applications.

## Acknowledgments

The authors would like to thank the Ministry of Higher Education Malaysia for financial support under the Fundamental Research Scheme (FRGS) No. FRGS/1/2023/TK10/UMP/02/37 (University reference RDU230135), Ministry of Education Malaysia, Ministry of Education Indonesia, University of Jember, and Universiti Malaysia Pahang Al-Sultan Abdullah for the facilities and support provided for this research.

## Funding

This work was supported by the Ministry of Higher Education Malaysia under the Fundamental Research Scheme (FRGS) No. FRGS/1/2023/TK10/UMP/02/37 (University reference: RDU230135).

## Declaration of Competing Interests

The authors declare no conflict of interest.

## CRediT Authorship Contribution Statement

Mochamad Edoward Ramadhan: Conceptualisation, Methodology, Investigation, Data curation, Writing-original draft.
Ahmad Najmuddin Ibrahim: Supervision, Project administration, Funding acquisition, Writing-review & editing.
Yasuhiro Fukuoka: Validation, Formal analysis, Resources, Visualisation, Writing-review & editing.

## Availability of Data and Materials

The data supporting the findings of this study are available upon request from the corresponding author.

## Ethics Declarations

This study did not involve human participants or animal subjects. Therefore, ethical approval was not required.

## Generative Artificial Intelligence Declarations

We declare that generative AI and AI-assisted technologies were not used to generate the content, ideas, or theories. AI tools were used solely to enhance the readability and refine the language. All outputs were carefully reviewed and approved, and we take full responsibility for the content of this manuscript.

## References


[1] Kubota T, Iizuka K, Nakane Y. Experimental study of wheel traction performance for planetary rovers with grousers. Journal of Terramechanics. 2003;40:123–135.

[2] Ishigami G, Miwa A, Nagatani K, Yoshida K. Terramechanics-based model for steering maneuver of planetary exploration rovers on loose soil. Journal of Field Robotics. 2007;24(3):233–250. https://doi.org/10.1002/rob.20187

[3] Nakashima Y, Fujii H, Oida A, Momozu M, Kanamori H, Aoki S, et al. Discrete element method analysis of single wheel performance for a small lunar rover on sloped terrain. Journal of Terramechanics. 2010;47(5):307–321. https://doi.org/10.1016/j.jterra.2010.04.001

[4] Irani F, Bauer RJ, Waller JP. A dynamic terramechanics model for rigid wheels with grousers on sandy soil. Journal of Terramechanics. 2011;48:1–14. https://doi.org/10.1016/j.jterra.2011.05.001

[5] Sutoh M, Nagaoka K, Nagatani K, Yoshida K. Influence of wheel parameters on mobility of planetary rovers on loose soil. Journal of Terramechanics. 2012;49:345–353. https://doi.org/10.1002/rob.21405

[6] Sutoh M, Nagaoka K, Nagatani K, Yoshida K. Design of wheels with grousers for planetary rovers traveling over loose soil. Journal of Terramechanics. 2013;50(5–6):345–353. https://doi.org/10.1016/j.jterra.2013.05.002

[7] Zhou F, Arvidson RE, Bennett K, Trease B, Lindemann R, Bellutta P, et al. Simulations of Mars rover traverses. Journal of Field Robotics. 2014;31(1):141–160. https://doi.org/10.1002/rob.21483

[8] Higa K, Moreland S, Skonieczny K, Wettergreen D. Measurement of two-dimensional normal stress distribution on a rigid wheel. Journal of Terramechanics. 2015;62:1–10. https://doi.org/10.1016/j.jterra.2015.04.001

[9] Du J, Hou J, Dun Y, et al. Influence of wheel width on drawbar pull under different slip ratios. Journal of Terramechanics. 2018;76:45–55. https://doi.org/10.1016/j.jterra.2018.04.005
[10] Jiang H, Gao X, Liu Y, et al. Validation of a physical wheel model using discrete element method simulations and lunar soil simulant. Advances in Space Research. 2018;62:1801–1812. https://doi.org/10.1016/j.jterra.2017.12.001
[11] Higa K, Skonieczny K, Wettergreen D. Grousers dominate traction generation for rigid wheels on sand. Journal of Terramechanics. 2019;85:39–57. https://doi.org/10.1016/j.jterra.2019.07.001
[12] Inotsume H, Moreland S, Skonieczny K, Wettergreen D. Effects of grouser parameters under longitudinal and lateral slip conditions. Journal of Terramechanics. 2019;85:59–72. https://doi.org/10.1016/j.jterra.2019.06.002
[13] Ibrahim AN, Aoshima S, Shiroma N, Fukuoka Y. The effect of assistive anchor-like grousers on wheeled rover performance over unconsolidated sandy dune inclines. Sensors. 2016;16(9):1507. https://doi.org/10.3390/s16091507
[14] Ibrahim AN, Fukuoka Y. Effect of assistive grouser mechanism on lightweight rover power consumption pattern on steep soft sand inclines. In: Lecture Notes in Mechanical Engineering. Singapore: Springer; 2018. p. 331–338. https://doi.org/10.1007/978-981-10-8788-2_30
[15] Sabarudin SS, Ibrahim AN, Fukuoka Y. Effect of grouser angle of attack on performance of adjustable robot wheel assistive grouser. In: Lecture Notes in Mechanical Engineering. Singapore: Springer; 2020. p. 1111–1117. https://doi.org/10.1007/978-981-15-0950-6_92
[16] Aziz INAC, Ibrahim AN, Basri I, Fukuoka Y. Rover wheel assistive grouser angle of attack effects on traction force in soft terrain. In: Proceedings of the IEEE International Colloquium on Signal Processing and Its Applications (CSPA); 2023, Malaysia. Piscataway (NJ): IEEE; 2023. p. 236–241. https://doi.org/10.1109/CSPA57446.2023.10087721
[17] Aziz INAC, Ibrahim AN, Basri I, Fukuoka Y. Rover wheel assistive grouser shape effects on traction force in flat soft terrain. In: Proceedings of the 2023 IEEE International Conference on Automatic Control and Intelligent Systems (I2CACIS); 2023, Malaysia. Piscataway (NJ): IEEE; 2023. p. 281–286. https://doi.org/10.1109/I2CACIS57635.2023.10193664
[18] Basri I, Aziz INAC, Ibrahim AN, Fukuoka Y. Investigation of wheel robot grouser width parameter effect on robot mobility in soft sand terrain using sand test bed. In: Lecture Notes in Networks and Systems. Singapore: Springer; 2024. p. 199–207. https://doi.org/10.1007/978-981-99-8819-8_16
[19] Takehana K, Kizaki S, Tanaka T, Uno K, Yoshida K. Comparison of lunar rover wheel performance in soils with different cohesive properties. Journal of Terramechanics. 2025;117:101011. https://doi.org/10.1016/j.jterra.2024.101011
[20] Dong X, Jin J, Jia Z, Qi Y, Chen T, He L, et al. Soil-plowing wheel with C-shaped grousers for enhanced drawbar pull on sandy terrain. Journal of Terramechanics. 2025;118:101045. https://doi.org//10.1016/j.jterra.2024.101002